PHYSICAL REVIEW B **71**, 064406 (2005)

Magnetic properties and critical behavior of random α-FeMnAl alloys: An Ising Monte Carlo study

J. Restrepo*
Grupo de Estado Sólido. Instituto de Física, Universidad de Antioquia, A. A. 1226, Medellín, Colombia

J. M. Greneche
Laboratoire de Physique de l'Etat Condensé, UMR CNRS 6087, Université du Maine, 72085 Le Mans, Cedex 9, France
(Received 29 April 2004; revised manuscript received 13 October 2004; published 18 February 2005)

The effect of atomic disorder, dilution, and competing interactions upon the magnetic properties of α-FeMnAl alloys with different stoichiometries is addressed by means of the Monte Carlo method. Magnetization per site, specific heat, and magnetic susceptibility were computed as a function of temperature on the basis of a Metropolis dynamics, from which critical exponents were estimated. Simulation was carried out in the frame of a random site-diluted three-dimensional Ising model with nearest-neighbor interactions, where Fe-Fe ferromagnetic and Fe-Mn, Mn-Mn antiferromagnetic interactions, as well as the Al dilutor effect, were taken into account. Results, which are summarized in a magnetic phase diagram, reveal the occurrence of several phases including reentrant and pure spin-glass behaviors below around 11 K, and a ferromagnetic to paramagnetic phase transition at temperatures between 100 K and 400 K. Finally, critical exponents, which are consistent with Harris criterion, are also compared to those obtained in other 3D random Ising models.

DOI: 10.1103/PhysRevB.71.064406 PACS number(s): 75.50.Bb, 75.50.Lk, 75.40.Mg

I. INTRODUCTION

The effect of atomic disorder upon the magnetic properties and critical behavior of intermetallic crystalline compounds has been a topic of debate and long standing interest during the last decades. First, magnetic phase diagrams are strongly influenced by the degree of atomic ordering, i.e., they can be modified depending on the sample preparation method as it has been already reported to occur in FeAl (Refs. 1–4) and FeMnAl alloys.[5,6] Hence, experimental techniques like mechanical alloying and quenching after high-temperature treatments in arc-melted alloys, provide the mechanism for introducing atomic disorder.[5] Second, the existence of competing interactions and dilution (below or above the percolation threshold) increases the degree of complexity from which a wide variety of magnetic phases can be found. In a recent paper devoted to α-FeMnAl alloys[7] the temperature dependence of the mean hyperfine field B_{hf} from Mössbauer data for $Fe_{0.5}Mn_{0.1}Al_{0.4}$ reveal a well-distinguishable low-temperature region below 30 K, where the system exhibits a kink characterized by a sharp increase of B_{hf} from 10 T up to 14 T as the temperature decreases. Such behavior was ascribed to a reentrant spin-glass (RSG) state within a ferromagnetic matrix arising from the interplay between ferromagnetic Fe-Fe bonds, antiferromagnetic Fe-Mn, Mn-Mn couplings, and to the dilution effect provided by Al atoms in a Fe-rich environment. It is particularly the interesting fact that with a relative small amount of Mn, just 10 at. %, and consequently a relative small density of antiferromagnetic bonds leading to competition, a RSG behavior can be evidenced. On the other hand, as thermal fluctuations become larger by increasing temperature above 30 K, B_{hf} goes from 10 T down to zero as the critical temperature T_C is reached at around 300 K, taking place a ferromagnetic to paramagnetic phase transition. These facts in addition to the debate about critical exponents of random Ising systems have motivated us to consider the α-FeMnAl system as a canonical example of disordered system. First, atomic site randomness can be easily achieved both computationally as well as experimentally either by mechanical alloying or by quenching after arc melting.[5,6] Additionally, competing interactions responsible for frustration come from the ferromagnetic and the antiferromagnetic character of Fe-Fe and Fe-Mn, Mn-Mn couplings, respectively.[8–10] This fact gives rise to an exchange integral disorder which in turn is enhanced by the magnetically dilutor effect of Al atoms providing the so-called bond randomness. More important is perhaps the influence of such a level of disorder (atomic, magnetic, and diluted) upon the critical exponents, which remains a subject of much interest. Consequently, in this work we investigate the effect of dilution via Al as well as the effect of competing bonds via Mn on the magnetic properties and critical behavior of quenched-random α-FeMnAl alloys. More concretely, we have considered the following alloys series: $Fe_{0.7-x}Mn_xAl_{0.3}$, $Fe_{0.6-x}Mn_xAl_{0.4}$, and $Fe_{0.5-x}Mn_xAl_{0.5}$, corresponding to a body-centered-cubic (bcc) structure according to the structural phase diagram.[11] A Monte Carlo-metropolis dynamics and a random site-diluted three-dimensional (3D) Ising Hamiltonian with nearest-neighbors interactions have been considered for addressing the present study.

The layout of the paper is as follows. In Sec. II we describe the model, simulation details and observables to be computed. In Sec. III we present our numerical results. This section provides the finite-size scaling analysis of the $Fe_{0.5}Mn_{0.1}Al_{0.4}$ sample and it shows how the observed magnetic behavior is modified depending on stoichiometry accordingly to the above mentioned series. Results are summarized in a proposal of magnetic phase diagram. Conclusions are finally presented in Sec. IV.

II. MODEL

The zero-field random Ising Hamiltonian describing our system reads as follows:

$$H = -\sum_{\langle i,j \rangle} J_{ij}\varepsilon_i\varepsilon_j\sigma_i\sigma_j. \quad (1)$$

The sum runs over nearest neighbors, σ_i takes on the values +1, and the ε_i's are uncorrelated quenched-random variables chosen to be 1 or 0 depending on whether the ith site is occupied by a magnetic atom (Fe, Mn) or a nonmagnetic one (Al), respectively, having a probability distribution given by

$$P(\varepsilon_{ij}) = p\,\delta(\varepsilon_{ij} - 1) + x\,\delta(\varepsilon_{ij} - 1) + q\,\delta(\varepsilon_{ij}), \quad (2)$$

where p, x, and q are the fractional concentrations of Fe, Mn, and Al, respectively, with $p+x+q=1$. In contrast to pure systems, the occurrence of atomic disorder, dilution, and the presence of different couplings (Fe-Fe, Fe-Mn, and Mn-Mn) having different magnitudes, makes the exchange integral J_{ij} a randomly distributed function, instead of a constant value function of the form

$$P(J_{ij}) = p^2\delta(J_{ij} - J) + x^2\delta(J_{ij} + \xi J) + 2px\,\delta(J_{ij} + \lambda J) + q(2 - q)\,\delta(J_{ij}). \quad (3)$$

In this expression the coefficient p^2, representing a bond density, gives the probability of having ferromagnetic Fe-Fe couplings with strength J. x^2 and $2px$ are the respective probabilities of antiferromagnetic Mn-Mn and Fe-Mn couplings with exchange integrals $-\xi J$ and $-\lambda J$, where $\xi(\approx 5\%)$ and $\lambda(\approx 3\%)$ are competitive parameters fitted to reproduce experimental features of these alloys.[12] The last coefficient $q(2-q)$ gives the probability of diluted bonds involving aluminum. Additionally, the larger atomic size of Al atoms gives rise to a remarkable lattice expansion,[2,6] from which the exchange integral becomes a function of aluminum as it has been described elsewhere.[12,13] Numerical values for the present study were taken from Ref. 12. The choice for Ising spins allows reproducing a case with strong uniaxial anisotropy while keeping computational efforts within reasonable limits. This choice is also motivated by the fact we are dealing with a complex system containing three different elements, two of them are magnetic (Fe, Mn) with different couplings, randomly distributed in a bcc lattice, and where the exchange integral is an Al-driven function of interatomic spacing. Additionally, different system sizes are also considered for extrapolation purposes and computation of critical exponents. Moreover, since we want to stress on the possible existence of a spin-glass state according to the already described characteristics of our system, this should be better checked with Ising spins for which frustration effects arising from competition are enhanced.[14]

For our simulation we have employed a single-spin flip metropolis Monte Carlo algorithm[15,16] to study $L\times L\times L$ bcc lattices with periodic boundary conditions and several linear system sizes L ranging from 5 up to 25 with a total number of $N=2\times L^3$ atoms. The employed single-spin flip dynamics instead of, e.g., a single-cluster update is motivated by the high degree of dilution in our system where most probably one can find groups of spins almost completely surrounded by magnetic holes as a consequence of atomic disorder. In our case, this role of magnetic holes is played by Al atoms. Atomic disorder was simulated by considering up to ten different random quenched distributions of Fe, Mn, and Al atoms for every considered stoichiometry from which configurational averages over the ensemble ones and computation of error bars were carried out. Simulated annealing from well above the Curie temperature down to 1 K was carried out by starting from a random spin configuration corresponding to infinite temperature. In computing equilibrium averages, an average of 10^4 Monte Carlo steps per spin were considered after equilibration. The basic thermodynamic quantities of interest are the total energy E computed from Eq. (1) and the magnetization per lattice site $m=(1/N)\Sigma\sigma_i$ from which the specific heat c and the magnetic susceptibility χ were computed according to[15,16]

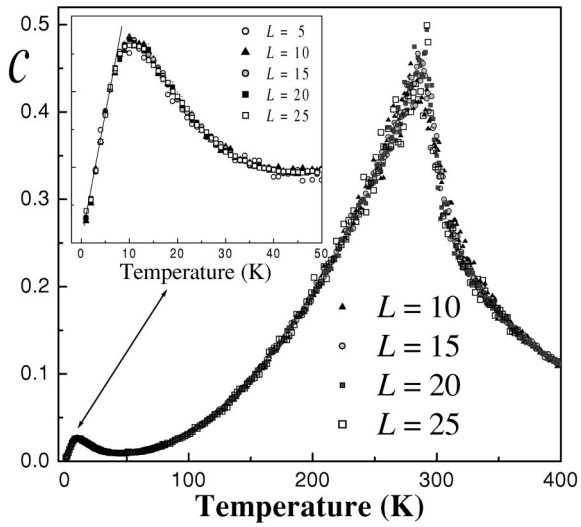

FIG. 1. Temperature dependence of the specific heat for $Fe_{0.5}Mn_{0.1}Al_{0.4}$. A lambda-type behavior around 300 K is observed corresponding to a ferromagnetic to paramagnetic transition. Inset shows the low-temperature behavior consistent with a spin-glass behavior.

$$c = (1/Nk_BT^2)(\langle E^2\rangle - \langle E\rangle^2), \quad (4)$$

$$\chi = (N/k_BT)(\langle m^2\rangle - \langle |m|\rangle^2), \quad (5)$$

which were in turn averaged over the number of samples, i.e., the number of random quenched distributions. Magnetic contributions to the total magnetization per site from Fe and Mn atoms were analyzed separately by considering $m_{Fe}=(1/N)\Sigma\sigma_{Fe}$ and $m_{Mn}=(1/N)\Sigma\sigma_{Mn}$, respectively. Replacing in Eq. (5) m by m_{Fe} or m_{Mn} the respective contributions χ_{Fe} and χ_{Mn} to the total susceptibility were also computed. This fact constitutes one of the enormous advantages of the Monte Carlo method compared to bulk magnetic measurements.

III. RESULTS AND DISCUSSION

Figure 1 shows the temperature dependence of the specific heat for the $Fe_{0.5}Mn_{0.1}Al_{0.4}$ sample. A well-defined

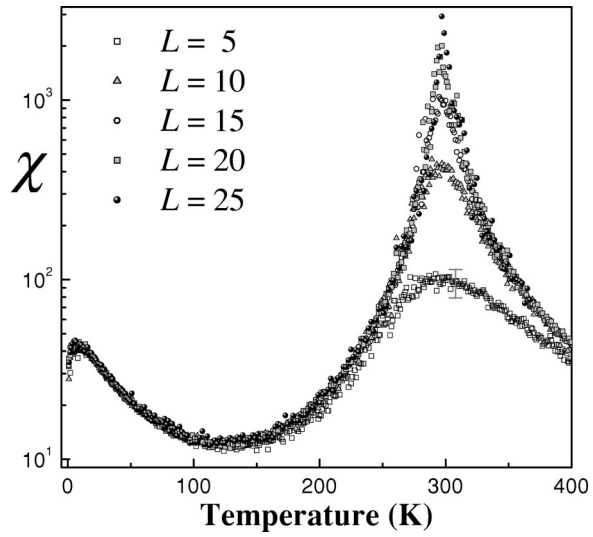

FIG. 2. Semilog plot of the temperature dependence of the magnetic susceptibility for $Fe_{0.5}Mn_{0.1}Al_{0.4}$. Two peaks are distinguishable in agreement with specific-heat results.

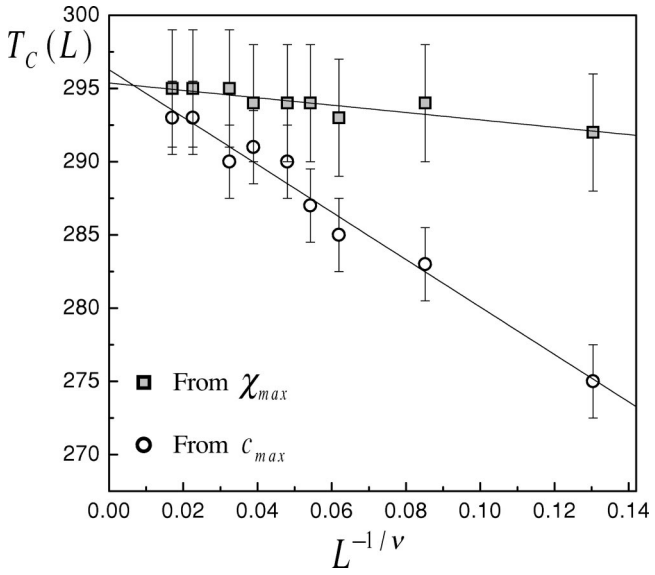

FIG. 3. Infinite volume extrapolation of the pseudocritical temperature $T_C(L)$ computed from specific-heat and magnetic susceptibility data.

lambda-type behavior around the Curie temperature ascribed to a thermal-driven ferromagnetic to paramagnetic phase transition and a small rounded peak in the low-temperature regime are observed. The presence of two peaks, one of them with tendency to diverge, is also endorsed by magnetic susceptibility data as can be observed in Fig. 2. Hence and from the location of the maxima of these quantities, denoted by $T_C(L)$, an extrapolation to the thermodynamic limit was carried out in the frame of finite-size scaling theory[15–18] with

$$T_C(L) \approx T_C(\infty) + aL^{-1/\nu}. \tag{6}$$

The best estimate for the Curie temperature was $T_C(\infty)=296\pm3$ K in agreement with Mössbauer results ($\sim$300 K) for this composition.[6,7,12] The extrapolation procedure is shown in Fig. 3 and it was carried out employing an effective correlation length exponent $\nu=0.79\pm0.03$. This exponent was estimated over the range $10^{-3}<|T/T_C-1|<10^{-2}$ from the maximum values of the logarithmic derivatives of the magnetization $|m|$ and the square of the magnetization m^2, following the procedure described by Ferrenberg and Landau.[17] The log-log plot of the size dependence of the maximum values of these derivatives used to determine ν is shown in Fig. 4. Our result for the correlation length exponent agrees with the 0.78 ± 0.01 value obtained by Hennecke[19] for the highly dilute Ising model with 60% of nonmagnetic sites on the basis of a finite-size scaling and renormalization analysis of Monte Carlo data. It also agrees with the 0.77 ± 0.04 value found by Wang and Chowdhury from a Monte Carlo analysis of the random Ising model[20] with a nonmagnetic sites concentration between 20% and 60%. Similar values have also been found experimentally for some site-random Ising systems. Concretely, for $Mn_{0.5}Zn_{0.5}F_2$, an exponent $\nu=0.75\pm0.05$ computed from neutron-scattering experiments has been reported.[21] A comparable value of 0.73 ± 0.03 was also found by Birgeneau *et al.*[22] for $Fe_{0.5}Zn_{0.5}F_2$ from neutron-scattering and linear birefringence measurements. Concerning the β exponent, Fig. 5 shows the temperature dependence of the magnetization per lattice site for the $Fe_{0.5}Mn_{0.1}Al_{0.4}$ alloy, whereas the inset shows the log-log plot of the magnetization evaluated at the extrapolated Curie temperature for different L values. From the slope and according to Refs. 15–18

$$[\langle|m(T_C(\infty))|\rangle] \propto L^{-\beta/\nu}, \tag{7}$$

our best estimate for β is 0.39 ± 0.05, reasonably similar within the error bars to those values reported by several authors on quenched dilute Ising systems as can be observed in the works and compilations made recently by Ballesteros *et al.*[23] and Folk *et al.*[24] More concretely, this value agrees with

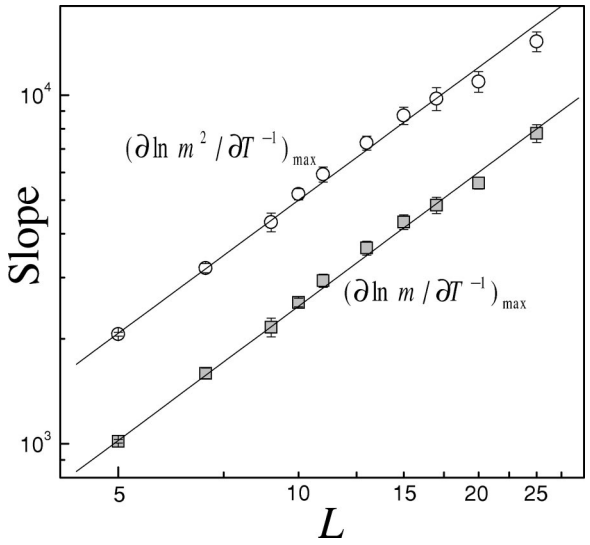

FIG. 4. Log-log plot of the size dependence of the maximum values of the logarithmic derivatives of the magnetization and the square of the magnetization to determine ν.

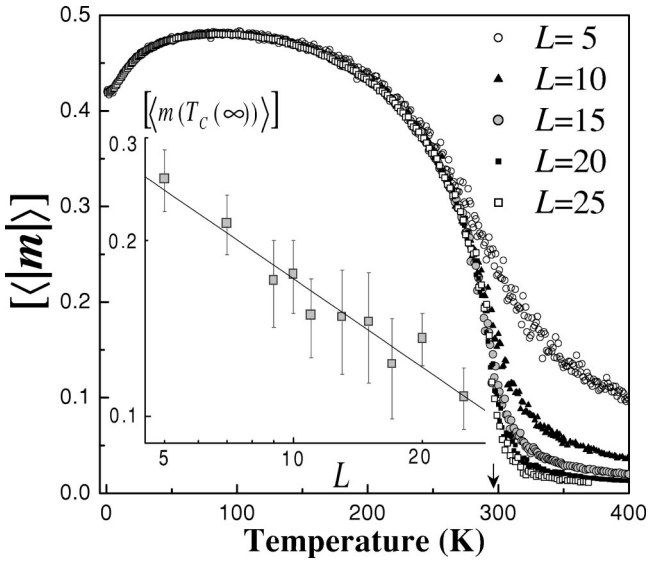

FIG. 5. Total magnetization per lattice site. Symbols $\langle\cdots\rangle$ and $[\cdots]$ refer to canonical ensemble and configurational averages, respectively. Inset is a log-log plot of the magnetization evaluated at the extrapolated Curie temperature.

$\beta=0.385\pm0.015$ for 20% of dilution, obtained by Marro *et al.* on Ising models with static site dilution.[25] With the obtained values for ν and β, the scaling plot of the rescaled value of the magnetization $mL^{\beta/\nu}$ as a function of $tL^{l/\nu}$ with $t=(T\text{-}T_C)/T_C$ is presented in Fig. 6 revealing the collapse onto a single curve for system sizes greater than ten. Analogously we have computed the critical exponent γ of the susceptibility from the double logarithmic plot of the size dependence of the maximum value of this function as shown in Fig. 7. From the slope we find $\gamma/\nu=2.00\pm0.05$ yielding the exponent $\gamma=1.58\pm0.10$ larger than most of the γ values reported in literature[23,24] for the dilute Ising model. Neverthe-

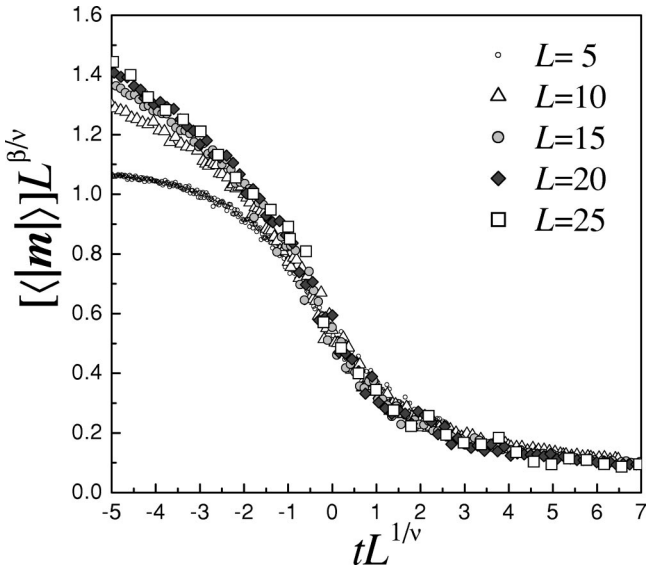

FIG. 6. Scaling plot of the rescaled absolute value of the magnetization $mL^{\beta/\nu}$ as a function of $tL^{1/\nu}$, with $\nu=0.79$ and $T_C=296$ K. Error bars are of the order of symbol size.

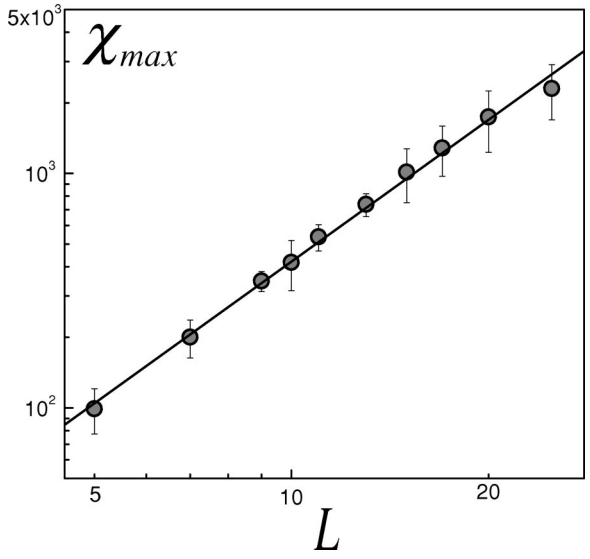

FIG. 7. Log-log plot of the maximum value of the magnetic susceptibility as a function of the linear system size to determine γ.

less, our estimate is similar to $\gamma=1.52\pm0.07$ reported by Wang and Chowdhury,[20] and 1.522 ± 0.031 for 40% of dilution as in our sample, found by Wiseman and Domany.[26] Regarding the ratio γ/ν, our estimate agrees well with the value 2.034 ± 0.031 found by Wiseman and Domany[26] and it is relatively close to renormalization-group calculations for which $\gamma/\nu=1.97$.[27,28] The observed fluctuations over the considered range of temperature on the specific-heat data, very sensitive to the length of the simulations, make more difficult to analyze the singular behavior of the specific heat. Assuming in this case the hyperscaling relation $\alpha+d\nu=2$ we found $\alpha=-0.37\pm0.09$, much more negative than most of those reported in literature[23,24] usually between -0.09 and -0.17. However, it agrees with those obtained from the same hyperscaling relation, namely, -0.34 and -0.31, in Refs. 19 and 20, respectively. Clearly the obtained exponents differ markedly from the pure Ising values. This fact, consistent with Harris argument, suggests therefore the occurrence of a random Ising behavior. On this respect it is important to stress that the degree of disorder in our system is provided not only by the site randomness over which most of the reported work on random Ising models focuses on but also by the bond randomness as a consequence of the distributed character of the exchange integrals accordingly with Eq. (3). These features in addition to the competitive character of the involved couplings (Fe-Fe, Fe-Mn, Mn-Mn) of different magnitudes and different sign ($J_{\text{Fe-Fe}}>0, J_{\text{Fe-Mn}}<0, J_{\text{Mn-Mn}}<0$), enhance the degree of disorder in the system. This fact could presumably explain differences among sets of critical exponents since as is well established a crossover to new critical behavior is governed by the degree of scattering of the exchange integrals.[22] Regarding the nature of the low-temperature peak observed in Fig. 1, this is attributed to the presence of Mn atoms and more specifically to the Fe-Mn and Mn-Mn antiferromagnetic interactions competing with the Fe-Fe ferromagnetic ones. Moreover, in agreement with the third law of thermodynamics, the specific heat linearly tends to zero as

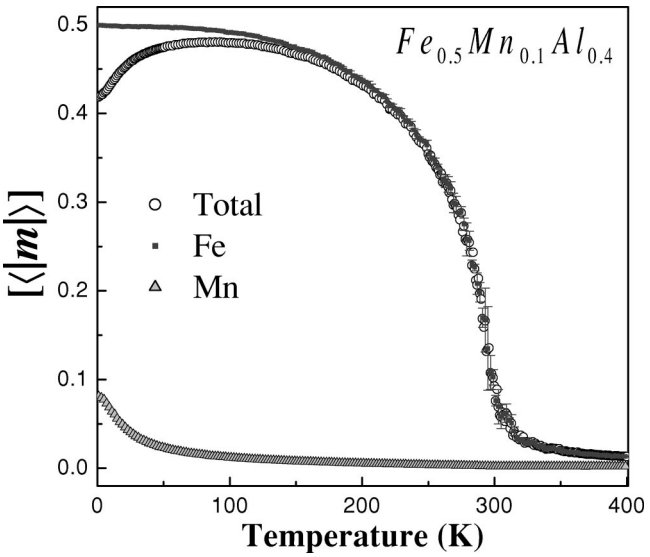

FIG. 8. Iron and manganese contributions to the total magnetization per site for $Fe_{0.5}Mn_{0.1}Al_{0.4}$, and $L=20$.

the temperature goes to zero. Such a linear dependence seems to be typical of spin-glass systems.[14,29] It is also a remarkable fact that this low-temperature behavior is evidenced with just 10 at. % Mn in agreement with experimental results[5–7] and it is correlated with a reduction in the global magnetization per site as observed in Fig. 5. In order to get a better understanding about this low-temperature behavior and why the low-temperature peak in the specific heat as well as in the susceptibility can be indeed ascribed to those antiferromagnetic interactions involving Mn, we show explicitly the Fe and Mn contributions to the global magnetization per site and to the susceptibility for $L=20$ in Figs. 8 and 9, respectively. Results reveal clearly a remarkable increase of the absolute value of the contribution due to Mn atoms in contrast to the Fe magnetization contribution which

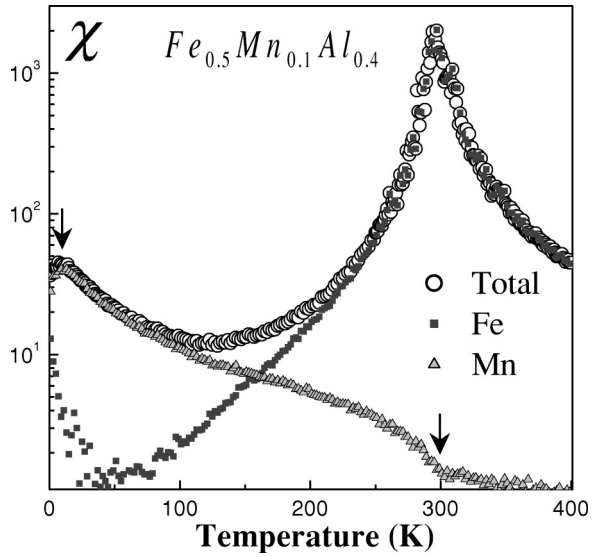

FIG. 9. Semilog plot of the total susceptibility and its respective contributions for $Fe_{0.5}Mn_{0.1}Al_{0.4}$ and $L=20$. Arrows indicate the position of critical points.

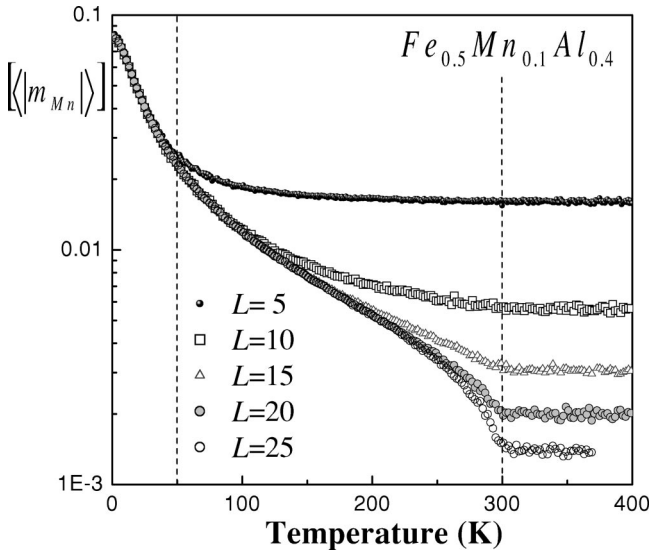

FIG. 10. Semilog plot of the manganese contribution to the magnetization as a function of temperature for different linear system sizes.

remains practically constant. This result implies therefore a low-temperature additional ordering of Mn spins within the ferromagnetic matrix. A detailed analysis of this curve, as can be seen more explicitly in the semi-log plot of Fig. 10 for different system sizes, shows that the observed Mn magnetization per site (0.08) as temperature goes to zero differs from that suggested by stoichiometry (0.1). This fact means that a fraction of about 20% of Mn magnetic moments tend to be randomly oriented, some of them presumably becoming frustrated as a consequence of the involved competing interactions. In contrast, around 80% of the Mn magnetic moments are antiferromagnetically coupled to the Fe-rich ferromagnetic matrix. Since this behavior arises within the ferromagnetic phase below the Curie temperature, a reentrant spin-glass behavior is concluded. In this way, the antiferromagnetic Fe-Mn coupling makes the global magnetization to decrease. Such a decrease has been in fact already reported to occur in $Fe_{0.5}Mn_{0.1}Al_{0.4}$ alloys by means of superconducting quantum interference device magnetometry and magnetic susceptibility measurements.[6] As the Mn concentration increases up to 20 at. % without changing the Al content, which corresponds to increase the number of antiferromagnetic bonds and therefore the density of competing bonds, the fraction of Mn moments becoming frustrated increases. This situation is clearly observed in Fig. 11 for the $Fe_{0.4}Mn_{0.2}Al_{0.4}$ sample, for which an almost equiatomic distribution of Mn magnetic moments randomly oriented and antiferromagnetically coupled to the Fe ferromagnetic matrix is obtained. It must be stressed that only a fraction of those Mn magnetic moments randomly oriented must be indeed frustrated since the presence of small diluted clusters containing a considerable amount of Mn cannot be discarded as a consequence of atomic disorder. This phenomenology coincides with a higher peak of the specific heat in the low-temperature regime and it becomes progressively more relevant as the Mn content increases. On the other hand as observed in Fig. 11, the contribution to the magnetization

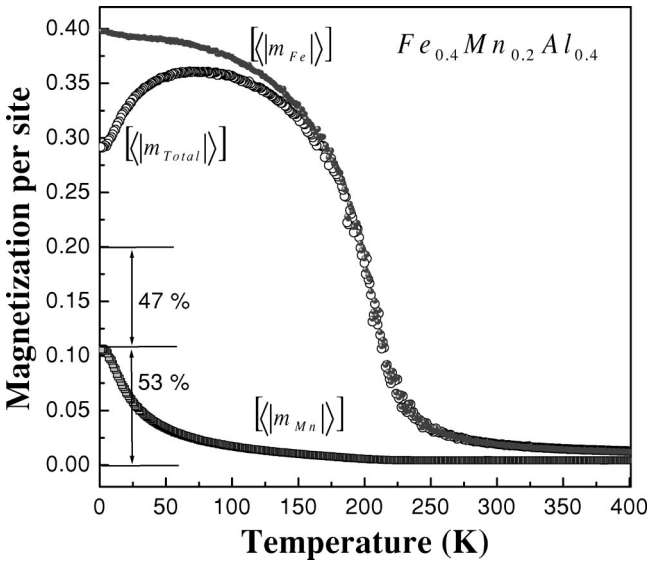

FIG. 11. Iron and manganese contributions to the total magnetization per site as a function of temperature for $Fe_{0.4}Mn_{0.2}Al_{0.4}$ and $L=20$.

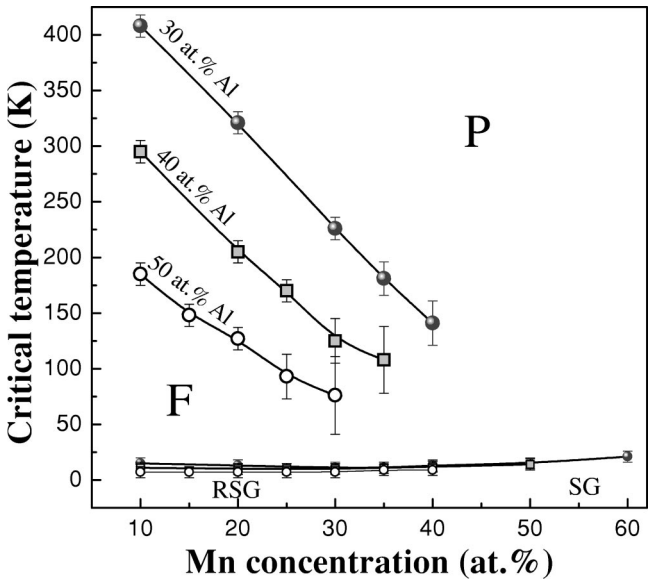

FIG. 13. Magnetic phase diagram of α-FeMnAl random Ising alloys. Labels correspond to the following states: F, Ferromagnetic; P, Paramagnetic; RSG, Reentrant spin-glass; and SG, spin glass.

from iron atoms as the temperature goes to zero, seems to suggest a very small additional increase of this contribution attributed to a reduction of thermal fluctuations in a weaker ferromagnetic matrix, i.e., characterized by a lower density of ferromagnetic bonds. Figure 12 shows the effect of the Mn content on the temperature dependence of the specific heat for the $Fe_{0.6-x}Mn_xAl_{0.4}$ series. As is shown in this figure, Curie temperature is shifted with manganese toward lower values, attributed to a smaller density of ferromagnetic bonds and to the increasingly density of antiferromagnetic bonds for which the Fe-Mn and Mn-Mn couplings are smaller in magnitude than the corresponding to pure iron,[12] i.e., $J_{\text{Fe-Mn}}=-0.03\ J_{\text{Fe-Fe}}$, and $J_{\text{Mn-Mn}}=-0.05\ J_{\text{Fe-Fe}}$. Moreover, according to Eq. (3), an increase in the Mn content shifts the

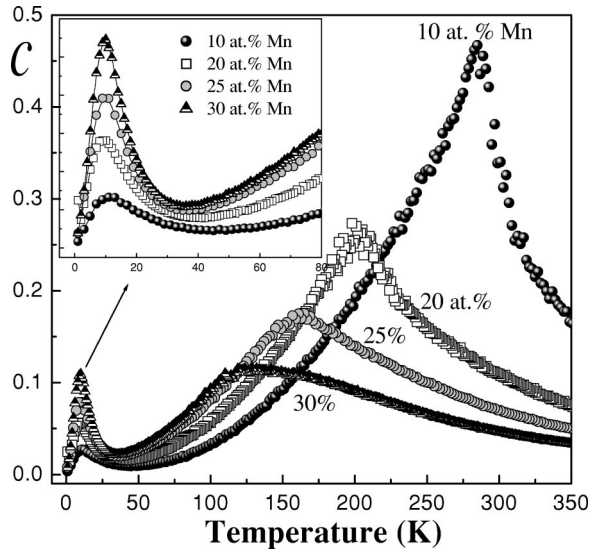

FIG. 12. Temperature dependence of the specific heat for different Mn concentrations corresponding to the $Fe_{0.6-x}Mn_xAl_{0.4}$ alloy series.

exchange integral distribution function and consequently the specific-heat peak, which in turn decreases in magnitude. This scenario in addition to the considered levels of dilution and the increasingly probability of clusters containing Mn, suggest a distribution of critical temperatures, i.e., a distribution of lambda curves. Such distribution is responsible for the broadening and rounded peak of the specific heat as the Mn content is increased. In contrast, the intensity of the low-temperature peak increases with the Mn concentration without practically changing its position. Such a compositional insensitivity of the freezing temperature has been in fact reported to occur in $Fe_{0.6-x}Mn_xAl_{0.4}$,[7] $Fe_{0.9-x}Mn_{0.1}Al_x$,[5,6] and $Fe_xMn_{0.7-x}Al_{0.3}$[30] disordered alloys. On this respect, the freezing temperature was estimated in around 11 K from the local maximum of the magnetic specific heat in the low-temperature regime. The reason for the compositional invariance of the freezing temperature can be understand in the mean-field approximation as a consequence of the small values of the Mn-Mn and Mn-Fe interactions compared to the Fe-Fe interactions. At low temperature, in the ordered Fe matrix, the freezing critical temperature for 40 at. % Al can be written as $T_f=zxJ_{\text{Mn-Mn}}+z(0.6-x)J_{\text{Fe-Mn}}$, where $z=8$ is the coordination number in our bcc lattice. By replacing the exchange integrals in terms of $J_{\text{Fe-Fe}}$, the differences for the freezing temperature due to composition are given approximately by $0.16xJ_{\text{Fe-Fe}}$ which is always very small compared to $J_{\text{Fe-Fe}}$. Thus for $x=0$ and $x=0.3$ (the maximum value of Mn considered) the difference comes out $0.048J_{\text{Fe-Fe}}$, which is negligible compared to $J_{\text{Fe-Fe}}$. Summarizing the obtained results, we propose the magnetic phase diagram shown in Fig. 13. First, a closely linear decrease of the Curie temperature with the Mn content at concentrations between 10 at. % and 40 at. % Mn is observed. Second, a RSG phase and a pure spin-glass behavior depending on Mn content below around 11 K as shown in Fig. 13 are also evidenced. As the Mn concentration is increased as shown in Fig. 12, the broad

and rounded peak in the specific heat at around T_C, for which the lambda-type behavior is progressively no longer observed, makes the phase transition something gradual due to the increasingly probability of having distributions of clusters containing Mn with different local transition temperatures. Moreover, the occurrence of a cluster glasslike state cannot be discarded as a consequence of the high levels of dilution (up to 50 at. % Al) giving rise to fine magnetic clusters separated each other by Al-rich regions. At much higher Mn concentrations beyond those considered in the present work, leading to a Mn-rich matrix as well as to structural changes, the magnetic behavior should be finally determined by the antiferromagnetic character of interactions involving manganese.

IV. CONCLUSIONS

The effects of dilution and the presence of competing interactions in a matrix exhibiting ferromagnetic characteristics have been considered. They play an important role in determining the magnetic structure, and more concretely the reentrant spin-glass and pure spin-glass behaviors of a disordered system such as those considered in the present study. The obtained results based on α-FeMnAl disordered alloys revealed that a fraction of the total number of Mn spins become frozen at a freezing temperature practically insensitive to Mn composition at around 11 K in agreement with experimental results. A thermal-driven ferromagnetic to paramagnetic phase transition with a Curie temperature decreasing with the Mn content as proposed in the magnetic phase diagram shown in Fig. 13 is also reported. Such behavior is ascribed to the smaller strength of the antiferromagnetic interactions Fe-Mn and Mn-Mn as compared to the ferromagnetic ones. Additionally from magnetic specific-heat data, a smooth evolution between a well-defined lambda-type behavior at around T_C and a broadened and rounded peak as the Mn content increases was also evidenced. This feature is attributed to the presence of clusters with different local concentrations due to atomic disorder giving rise to a distribution of transition temperatures. Concerning the critical behavior, critical exponents of the ferromagnetic-paramagnetic transition were analyzed for the particular composition $Fe_{0.5}Mn_{0.1}Al_{0.4}$, revealing the occurrence of random exchange Ising behavior consistent with Harris argument. Finally, the employed Ising-Monte Carlo approach provides a satisfactory description of the variable-temperature magnetic properties of the FeMnAl disordered system and reveals additional information which is not currently available from experiment like those contributions to the magnetization and to the magnetic susceptibility of the involved magnetic elements (Fe, Mn) in a differentiated fashion.

ACKNOWLEDGMENTS

This work was supported by University of Antioquia in the frame of the Sostenibilidad Project No. IN5222CE of the Solid Sate Group, the COLCIENCIAS Project No. 1115-05-12409, and the ECOS-Nord Project No. C03P01. One of the authors (J.R.) would like to thank the one year postdoctoral fellowship provided by the Région Pays de la Loire at the Université du Maine-Le Mans (France). Simulations were performed on the Lotus cluster of Université du Maine, LPEC (web site: http://weblotus.univ-lemans.fr/w3lotus).

*Email address: jrestre@fisica.udea.edu.co

[1] F. Schmid and K. Binder, J. Phys.: Condens. Matter **4**, 3569 (1992).
[2] G. A. Pérez Alcázar and E. Galvão da Silva, J. Phys. F: Met. Phys. **17**, 2323 (1987).
[3] X. Amils, J. S. Garitaonandia, J. Nogués, S. Suriñach, F. Plazaola, J. S. Muñoz, and M. D. Baró, J. Non-Cryst. Solids **287**, 272 (2001).
[4] E. Apiñaniz, J. S. Garitaonandia, and F. Plazaola, J. Non-Cryst. Solids **287**, 302 (2001).
[5] J. Restrepo, G. A. Pérez Alcázar, and J. M. González, Hyperfine Interact. **134**, 27 (2001).
[6] J. Restrepo, G. A. Pérez Alcázar, and J. M. González, J. Appl. Phys. **87**, 7425 (2000).
[7] C. González, G. A. Pérez Alcázar, L. E. Zamora, J. A. Tabares, and J. M. Greneche, J. Phys.: Condens. Matter **14**, 1 (2002).
[8] H. Bremers, Ch. Jarms, J. Hesse, S. Chadjivasiliou, K. G. Efthimiadis, and I. Tsoukalas, J. Magn. Magn. Mater. **63**, 140 (1995).
[9] M. A. Kobeissi, J. Phys.: Condens. Matter **3**, 4983 (1991).
[10] J. Restrepo and G. A. Pérez Alcázar, Phys. Rev. B **61**, 5880 (2000).
[11] D. J. Chakrabarti, Metall. Trans. B **8B**, 121 (1977).
[12] J. Restrepo, O. Arnache, and D. P. Landau, Physica B **320**, 239 (2002).
[13] G. A. Pérez Alcázar, J. A. Plascak, and E. Galvão da Silva, Phys. Rev. B **34**, 1940 (1986).
[14] K. Binder and A. P. Young, Rev. Mod. Phys. **58**, 801 (1986).
[15] D. P. Landau and K. Binder, *A Guide to Monte Carlo Simulations in Statistical Physics* (Cambridge University Press, Cambridge, 2000), p. 71.
[16] M. E. J. Newman and G. T. Barkema, *Monte Carlo Methods in Statistical Physics* (Clarendon, Oxford, 1999), p. 46.
[17] Alan M. Ferrenberg and D. P. Landau, Phys. Rev. B **44**, 5081 (1991).
[18] Michael E. Fisher and Michael N. Barber, Phys. Rev. Lett. **28**, 1516 (1972).
[19] Michael Hennecke, Phys. Rev. B **48**, 6271 (1993).
[20] J.-S. Wang and D. Chowdhury, J. Phys. (France) **50**, 2905 (1989).
[21] P. W. Mitchell, R. A. Cowley, H. Yoshizawa, P. Böni, Y. J. Uemura, and R. J. Birgeneau, Phys. Rev. B **34**, 4719 (1986).
[22] R. J. Birgeneau, R. A. Cowley, G. Shirane, H. Yoshizawa, D. P. Belanger, A. R. King, and V. Jaccarino, Phys. Rev. B **27**, 6747 (1983).
[23] H. G. Ballesteros, L. A. Fernandez, V. Martin-Mayer, A. Munoz Sudupe, G. Parisi, and J. J. Ruiz-Lorenzo, Phys. Rev. B **58**, 2740 (1998).

[24] R. Folk, Yu. Holovatch, and T. Yavors'kii, Phys. Rev. B **61**, 15 114 (2000).
[25] J. Marro, A. Labarta, and J. Tejada, Phys. Rev. B **34**, 347 (1986).
[26] S. Wiseman and E. Domany, Phys. Rev. E **58**, 2938 (1998).
[27] I. O. Mayer, J. Phys. A **22**, 2815 (1989).
[28] H. K. Janssen, K. Oerding, and E. Sengespeick, J. Phys. A **28**, 6073 (1995).
[29] J. A. Mydosh, *Spin glasses: An Experimental Introduction* (Taylor & Francis, London, Washington D. C., 1993).
[30] Ligia E. Zamora, G. A. Pérez Alcázar, A. Bohórquez, J. F. Marco, and J. M. González, J. Appl. Phys. **82**, 6165 (1997).